

# Detecting Life-bearing Extra-solar Planets with Space Telescopes

v. 2

Steven V. W. Beckwith<sup>1,2</sup>

*Space Telescope Science Institute, 3700 San Martin Drive, Baltimore, MD 21218, USA*

svwb@stsci.edu

## ABSTRACT

One of the promising methods to search for life on extra-solar planets (exoplanets) is to detect life's signatures in their atmospheres. Spectra of exoplanet atmospheres at the modest resolution needed to search for oxygen, carbon dioxide, water, and methane will demand large collecting areas and large diameters to capture and isolate the light from planets in the habitable zones around the stars. For telescopes using coronagraphs to isolate the light from the planet, each doubling of telescope diameter will increase the available sample of stars by an order of magnitude, indicating a high scientific return if the technical difficulties of constructing very large space telescopes can be overcome. For telescopes detecting atmospheric signatures of transiting planets, the sample size increases only linearly with diameter, and the available samples are probably too small to guarantee detection of life-bearing planets. Using samples of nearby stars suitable for exoplanet searches, this paper shows that the demands of searching for life with either technique will require large telescopes, with diameters of order 10 m or larger in space.

*Subject headings:* techniques:miscellaneous — planetary systems — extraterrestrial intelligence — telescopes

## 1. INTRODUCTION

The detection of more than 200 planets outside the Solar System is a powerful incentive to search for extra-terrestrial life. Although extra-terrestrial life could take on many guises, economy of hypothesis (and a practical approach) implies that we should first search for signs of life similar to those seen on Earth. An advantage of using the Earth as a proxy for analysis is that it bounds the problem and provides concrete examples of signatures subject to passive detection, i.e. not requiring signals broadcast by sentient beings.

In the Earth's atmosphere, the chemical components have been altered by life. Evidence for life on Earth could be detected from afar in the spectral signatures of these molecules: oxygen, carbon dioxide, methane, and water vapor

(Sagan et al. 1993). The rise of photoplankton and plants on Earth created an atmosphere with a large reservoir of oxygen today that requires steady production by photosynthesis to maintain its present level, for example. If we could study the same spectral signatures in the atmospheres of exoplanets, we could search for signs of life similar to some of the earliest and most robust forms on our own planet (Seager et al. 2002; Kaltenegger et al. 2007). Chemical signatures of life on other planets would revolutionize our thinking about Earth's uniqueness and provide tantalizing evidence that we are not alone in the universe.

Observing exoplanets directly is difficult owing to their proximity to the much brighter stars that keep them warm. Although technically challenging, this problem is well understood, and there are a variety of strategies that can reduce the brightness of the starlight without diminishing the light from the planet for direct detection (Guyon et al. 2006; Cash 2006)

<sup>1</sup>Space Telescope Science Institute

<sup>2</sup>Johns Hopkins University

or use the star itself as a background source to probe the atmosphere when the exoplanet transits the face of the star (Charbonneau et al. 2002; Ehrenreich et al. 2006). The first technique must overcome diffraction in the pupil of the telescope, a well understood phenomenon, and it is possible to characterize the detection problem in general terms to understand the kinds of instruments that will be needed to study exoplanets and search for signs of life. The second technique depends only on the photometric accuracy of an observation and is easy to calculate for any star.

Any planet supporting life as on Earth must satisfy two broad criteria: (1) it must have surface temperatures in the range 273 to 373 K, where water is in the liquid phase, and (2) it must have an atmosphere. The first criterion is met if the planet is in the *habitable zone* (HZ) around the star, a range of orbital distances where the equilibrium temperature for a rotating body is between the freezing and boiling points of water. The second criterion is met if the planet is rocky and can retain an atmosphere; current estimates specify a between 0.5 to 10 Earth masses. Smaller planets will not retain their atmospheres, and larger planets accrete gas and become gas giants. Although these criteria are probably far too restrictive to encompass all the possibilities for other life forms in the universe—or even on Earth itself—they are the only ones amenable to remote observation with technology that we can foresee at present and thus provide a good basis for a targeted search.

There have been many calculations aimed at refining our ideas of the habitable zone (e.g. Kasting et al. 1993), suitable samples of stars to search (Turnbull & Tarter 2003; Turnbull 2004; Turnbull et al. 2006), and the impact of specific telescopes on such a search (Agol 2007), and there is some disagreement about the likelihood of success depending on the different assumptions used. Most authors to date concentrate on photometric detection alone, obviating the means to search for life. Agol (2007) treats the subject in considerable detail but focuses on the photometric detection problem.

However, the utility of using photometric searches alone to identify exoplanets for subsequent study could be obviated by the difficulty of measuring the orbits accurately enough to recover them at a later time (Brown 2005;

Brown et al. 2007). For apertures sizes under discussion for the Terrestrial Planet Finder (TPF) mission, habitable zones of most potential target stars are highly obscured. Most planets of interest will spend most of the time behind the central obscuration of the imaging instrument. To ensure efficient recovery of a newly discovered planet at future observing epochs, it will be necessary to accurately estimate the orbit from a small number of astrometric measurements. This implies a lower limit to the aperture size based on operational requirements (Brown et al. 2007). Achieving adequate astrometric may demand apertures larger than any so far discussed for TPF (Brown 2007, personal communication). If true, discovery and immediate spectroscopy of candidate sources near the stars may be the most efficient means of identifying those most interesting for follow up observations to determine if life is, indeed, present, making it essential to understand the spectroscopic requirements at the outset.

The purpose of this article is to derive the main scaling parameters for the study of life-bearing exoplanets in known samples of stars to understand the size of the telescopes needed for a robust search. We adopt simple but optimistic assumptions to bound the problem and find the minimum size for survey telescopes. Using only the lowest order approximations and assuming “best case” observing conditions allows robust conclusions about the scale of facilities needed to tackle the search for life.

The main premise is that direct photometric detection of exoplanets in a band where the exoplanet atmosphere is free of chemical signatures cannot be the endpoint of any mission to search for life-bearing planets; spectra of the atmospheres will be the major advance of observing the planets directly. Moreover, the rapid increase in the number of exoplanets discovered to date suggests that finding terrestrial planets will be easiest with indirect methods, such as observing radial velocity, photometric or astrometric variations in the host stars, and the real thrust of direct observations will be to search for signs of life.

## 2. Detecting Earth

The Earth’s flux density viewed from a distance is reasonably well constrained by its size and the

requirement that its equilibrium temperature is determined by external illumination at the temperature of the Sun. The same statements apply to exoplanets in the habitable zones around distant stars. An important result is that the flux densities of exoplanets in the habitable zones across a broad spectrum are roughly independent of the stellar luminosity and temperature.

If the exoplanet is a spherical body with radius,  $r_p$ , and temperature,  $T_p$ , and it is viewed at a distance,  $D \gg r_p$ , its thermal emission is at most that of a blackbody,  $B$ :

$$F_{pt}(\nu) = \frac{\pi r_p^2}{D^2} B(\nu, T_p), \quad (1)$$

The total emission is  $4\pi r_p^2 \sigma T_p^4$ .

The reflected light is in principle a rather complicated function of the planet's orbital phase and the detailed scattering properties of its atmosphere (e.g. Seager et al. 2000). For the purposes of this paper, it will be sufficient to assume the planet scatters like a Lambert sphere viewed at quadrature, the viewing angle  $\alpha = 90^\circ$ , with a fraction  $1 - a(\nu)$  of the light absorbed in the process. If it is illuminated by a star of radius,  $r_*$ , with an effective temperature,  $T_*$ , at orbital distance,  $R_p$ , from the star, the observed flux density of the reflected light is:

$$F_{pr}(\nu) = \frac{2}{3} \frac{r_p^2}{R_p^2} \phi(\alpha) a(\nu) \frac{\pi r_*^2}{D^2} \pi B(\nu, T_*), \quad (2)$$

$$= \frac{2}{3} a(\nu) \frac{r_p^2}{R_p^2} \frac{r_*^2}{D^2} \pi B(\nu, T_*), \quad (3)$$

where the Lambert sphere has a geometrical cross section of  $\frac{2}{3}$  and a phase function  $\phi(\alpha) = \frac{1}{\pi}(\sin \alpha + (\pi - \alpha) \cos \alpha) = \frac{1}{\pi}$  for  $\alpha = \frac{\pi}{2}$  (Russell 1916; Seager et al. 2000). The unabsorbed fraction,  $a(\nu)$ , will in general depend on frequency. For the Earth, it varies between  $\sim 0.7$  near  $0.3 \mu\text{m}$  to less than 0.3 longward of about  $0.6 \mu\text{m}$  and depends on variable factors such as cloud cover and exposed land mass (Kasting et al. 1993; Turnbull et al. 2006; McCullough 2006). We adopt  $a(\nu) = a = 0.5$  for the rest of this paper to produce a bright planet that should be most easily observed. As shown below, uncertainties in  $a(\nu)$  will not affect the estimates in this paper significantly. The actual spectra would also include

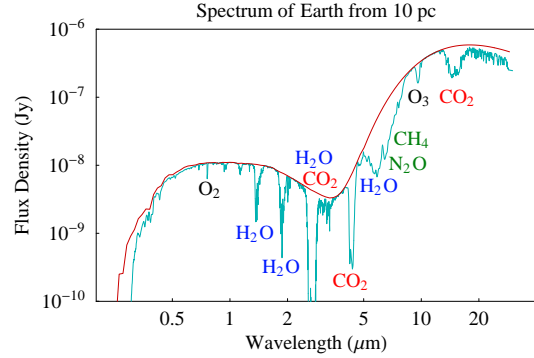


Fig. 1.— The green line is a synthetic spectrum of Earth viewed from 10 pc to illustrate the spectral features in the Earth's atmosphere. More exact models synthesized for different epochs in Earth's history show that spectra with resolution  $\Delta\nu/\nu$  of order 0.01 would allow the relative strengths of the organically produced molecules to be measured (Traub & Jucks 2002; Kaltenegger et al. 2007). The red line is a combination of the solar irradiance and a Planck function at 286 K.

radiative transfer effects in the atmosphere and show absorption lines from molecules (see Fig. 1).

Combining (1) and (3) with the assumptions above, the flux density of the planet is:

$$F_p(\nu) \approx \frac{\pi r_p^2}{D^2} \left( \frac{1}{3} \frac{r_*^2}{R_p^2} B(\nu, T_*) + B(\nu, T_p) \right). \quad (4)$$

This relation neglects some interesting details, such as the variable atmospheric transmission and radiative transfer effects as well as adopting assumptions about the albedo and phase function that are at best educated guesses. It turns out that these simplifications do not affect the overall energy balance enough to change the conclusions of this article, but they are, nevertheless, crucial for understanding the chemical composition of the planet's atmosphere.

At 10 pc, the apparent magnitude of the Earth at visual and near infrared wavelengths from (4) is about 29(AB),  $\sim 10 \text{ nJy}$ , too faint for spectra with any existing telescopes.

The principal sources of noise in detecting exoplanets will be local zodiacal light, any equivalent exo-zodiacal light in the other planetary system, any residual light from the star not cancelled by

the instrument, and the planet itself. Since we are interested in the limits of nature, we assume that starlight is completely eliminated by the telescope and instrument and consider only the other contributions.

The zodiacal light has the same spectrum as the Sun at wavelengths shorter than about  $3\mu\text{m}$ , but reduced by the optical depth of the zodiacal cloud in the direction of observation, and it is approximately a blackbody function at thermal infrared wavelengths with a temperature that depends somewhat on the viewing angle with respect to the Sun. The important point is that both the zody and exozody light will be uniform surface brightnesses to a good approximation whose observable fluxes depend only on the area–solid angle product (étendue) of the telescope and not the distance to the source. The spectrum of the zodiacal light combines a visual optical depth,  $\tau_z \sim 10^{-7}$ , and thermal emissivity,  $\epsilon_z(\nu) \sim 0.5$ , both strong functions of ecliptic line of sight, to obtain the brightness of the zodiacal light as:

$$I_z(\nu) \approx \tau_z [B(\nu, T_*) + \epsilon_z B(\nu, T_{\text{zody}})]. \quad (5)$$

It is straightforward to calculate the exact zodiacal emission in any direction from models in the literature (e.g. Leinert et al. 1998), and as a practical matter we will adopt a viewing angle at solar elongation  $90^\circ$  and ecliptic latitude  $45^\circ$  as “typical” of a large survey seeking to minimize zodiacal background:  $I_{\text{zody}}(\nu)$  is about  $0.3\text{ MJy sr}^{-1}$  at  $0.5\mu\text{m}$  and  $10\text{ MJy sr}^{-1}$  at  $10\mu\text{m}$ . Figure 2 compares the photon rates seen by 4 and 8 m telescopes from an Earth 10 pc away with the zodiacal light.

It is impossible to know how strong the contribution from the exo-zodiacal light is. It is easy to find stars with very large quantities of interplanetary dust (Beichman et al. 2006) and stars without detectable dust emission, so this term is one of the larger uncertainties in our estimates as stressed by Agol (2007). The best case is if there is no exo-zody at all. Alternatively, if the other planetary system is identical to the Solar System, the amount of exo-zody is just twice the local value. The easy way to understand this factor of 2 is to realize that we view the exo-zodiacal cloud through its entire thickness, whereas we reside at the mid-plane of the local zodiacal light (within  $3^\circ$ ) and thus look out through only half the optical depth in any direction. The exo-zodiacal

cloud will also be well resolved by any telescope with enough resolution to block the starlight to observe the planet. For the moment, we assume the contribution of the exo-zodiacal light is negligible.

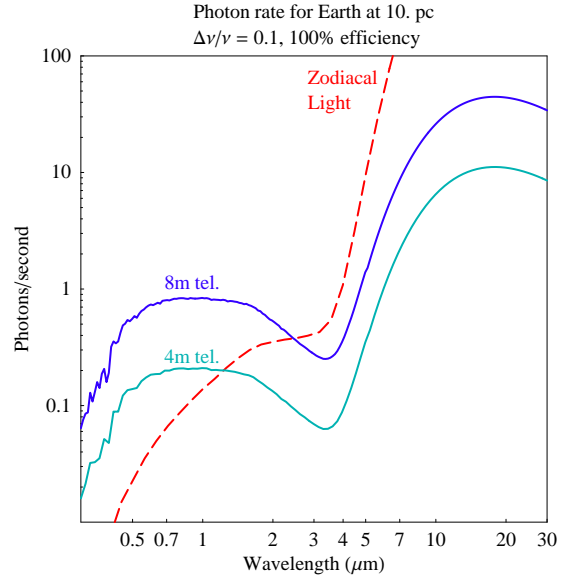


Fig. 2.— The photon rates for a photometric bandwidth ( $\Delta\nu/\nu = 0.1$ ) of an exo-Earth viewed from 10 pc distance with 4 m and 8 m telescopes, together with the photon rates for the local zodiacal light for a diffraction-limited telescope.

The noise of an observation will be dominated by the (Poisson) statistics of the incoherent photon stream from the planet and the zodiacal background. Denoting photon rates as  $\dot{N}_\gamma(p)$  and  $\dot{N}_\gamma(z)$ , respectively, the signal to noise ratio,  $SN$ , after observing time,  $t$ , is:

$$SN = \frac{\eta \dot{N}_\gamma(p)t}{(\eta \dot{N}_\gamma(p)t + \eta \dot{N}_\gamma(z)t)^{1/2}}, \quad (6)$$

$$= \sqrt{\eta t \frac{1}{h} \frac{\Delta\nu}{\nu}} \frac{A_{\text{tel}} F_p(\nu)}{\sqrt{A_{\text{tel}} (F_p(\nu) + \Omega_{\text{tel}} I_z(\nu))}}, \quad (7)$$

with the area and solid angle of the telescope denoted  $A_{\text{tel}}$  and  $\Omega_{\text{tel}}$ , and the overall detection efficiency  $\eta$ . For a circular telescope that is diffraction-limited, the étendue,  $A_{\text{tel}}\Omega_{\text{tel}}$ , is just equal to the square of the observing wavelength,

$\lambda^2$ . In the limit where the planet is far away, the photon noise is dominated by the zodiacal light regardless of whether it is local or around the exo-planet, since its contribution is independent of both source distance and telescope diameter, but the photon flux from the exo-planet is proportional to  $D^{-2}$ . Equation (7) may then be written as:

$$SN = t^{1/2} \sqrt{\frac{1}{h} \frac{\Delta\nu}{\nu}} \eta \frac{\frac{\pi}{4} d_{\text{tel}}^2 F_p(\nu)}{\sqrt{\left(\frac{c}{\nu}\right)^2 I_z(\nu)}}, \quad (8)$$

$$\propto t^{1/2} \left(\frac{d_{\text{tel}}}{D}\right)^2. \quad (9)$$

The expression in (9) shows the explicit dependence of  $SN$  and observation time on telescope diameter and source distance in the faint limit. If exo-zodiacal light is comparable in brightness to the local value,  $SN$  diminished by a factor of order  $\sqrt{3}$ . It is useful to note that even though the amount of exo-zodiacal light is uncertain, it introduces only a modest uncertainty into the signal-to-noise calculation considering many of the other uncertainties inherent in the planet detection problem. However, we will assume it is zero in subsequent calculations to consider the best case scenarios for detecting planets.

Recasting (8) in terms of observation time for Earth at a distance is especially useful for the planet detection problem:

$$t \approx 24 \text{ hr} \left(\frac{SN}{10}\right)^2 \frac{\nu/\Delta\nu}{100} \left(\frac{8 \text{ m}}{d_{\text{tel}}} \frac{D}{40 \text{ pc}}\right)^4 \quad (10)$$

assuming perfect efficiency,  $\eta = 1$ , and an observation wavelength  $\lambda = 1 \mu\text{m}$ .<sup>1</sup> Equation (10) shows that the time for an observation increases as the fourth power of distance over telescope diameter when observing a point source against a uniform brightness background in the photon limit. This strong dependence means that observations of Earth-like exoplanets with a telescope of a given size will be effectively limited to some maximum distance. Strictly speaking, these times are only valid for distances where the planet is fainter than

<sup>1</sup>Observations in the thermal infrared at wavelengths longer than a few microns allow relatively easy detection, but the challenges of starlight suppression considered in the next section are enormous, making single telescope observations unworkable.

the zodiacal light; for bright objects, the source flux itself also adds to the noise further increasing the required time. Figure 3 plots the times need to take low signal-to-noise spectra of an Earth at 10 pc with 4 and 8 m telescopes.

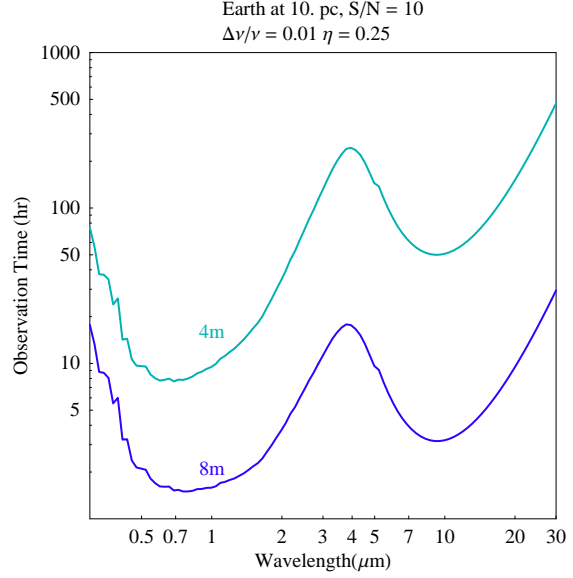


Fig. 3.— (Left): Integration time to achieve  $S/N=10$  for each spectral element for a practical 4 m and 8 m telescope at a resolving power of 100 assuming only background from the local zodiacal light; integration times would increase for any exo-zodiacal emission.

The assumptions used thus far assume a perfectly diffraction-limited telescope where the foreground radiation is dominated by zodiacal light. These conditions are easy to meet for a space telescope; they are extremely difficult to meet for any telescope on the Earth's surface. Even if the distortion of the wavefront from the Earth's atmosphere could be entirely compensated by an adaptive optics system, the atmosphere radiates strongly in all the lines of interest in Fig. 1 making the detection problem almost impossible for a ground-based telescope.

The practical effect of (10) is to limit the useful distance for observations of an exo-Earth with a given size telescope. It takes about 24 hr to take a spectrum of Earth at a distance of 40 pc with an 8 m telescope, a distance which shrinks to 27 pc, if the detection efficiency is 25%, typical for a good spectrograph. For a 4 m telescope, the lim-

iting distances for a 24 hr observation time are 20 and 13.5 pc, respectively, since the distance scales linearly with telescope diameter for this problem. These are large diameters for space telescopes. It is also useful to note the size of telescope below which the zodiacal light begins to dominate the light from the planet as a function of the distance to the planetary system,  $F_p(\nu) \leq \Omega_{\text{tel}} I_{\text{zody}}(\nu)$  in the denominator of (7). Using (4) and (5) at a wavelength of  $1 \mu\text{m}$ ,  $d_{\text{tel}} \leq 3.25 \text{ m } (D/10 \text{ pc})$ .

Sample volumes of the local neighborhood increase as the cube of the distance. Because there is a premium on maximizing the number of survey stars that can host potentially habitable planets, these results show a strong preference for large telescopes. The preferred size will depend on the density of suitable stars in the Solar neighborhood and their luminosity distribution to set the scale for the size of the habitable zones, the subject of the next section.

### 3. Number of Candidate Stars vs Telescope Size

The interesting candidate stars for any telescope will be those whose habitable zones can be resolved in the observation. Resolving the habitable zones means that the angular resolution of the telescope must be adequate to separate these regions from the star. Because the starlight must be essentially eliminated—the Sun is  $\sim 10^{10}$  times brighter than its reflected light from the Earth—starlight cancellation puts an even more stringent limit on the resolution, and it is a far higher technical hurdle than detection for exoplanet observations.

A telescope’s angular resolution is limited by diffraction at the pupil. The *inner working angle*,  $\theta_{IWA}$ , is normally defined as the smallest angular separation between a bright star and a much fainter planet at which the planet can be studied with good cancellation of the starlight. For a circular pupil, the diffraction pattern is an Airy function (Born & Wolf 1999), and  $\theta_{IWA}$  cannot be less than the distance to the first null at  $1.2\lambda/d_{\text{tel}}$ . Most realistic telescopes achieve inner working angles more than twice as large, even with nearly optimal designs (Guyon et al. 2006). The angle of the first null is typically a few tens of milli-seconds of arc:

$$1.2\lambda/d_{\text{tel}} = 0.21 \text{ arcsec } (\lambda/1 \mu\text{m}) (d_{\text{tel}}/1 \text{ m})^{-1}.$$

Almost all the interesting spectral features in the Earth’s atmosphere are longward of  $0.7 \mu\text{m}$  (Fig. 1.) A spectrum should extend to at least  $1 \mu\text{m}$  to be analyzed for evidence of disequilibrium chemistry indicative of life, and longer wavelengths bring in even more interesting features. We adopt  $\lambda = 1 \mu\text{m}$  as the minimum working wavelength to look for signs of life in spectra and the maximum wavelength to accommodate a small  $\theta_{IWA}$ .

The habitable zone can be calculated from the stellar luminosity. The total thermal emission,  $4\pi r_p^2 \sigma T_p^4$ , must equal the total amount of absorbed starlight,  $(1-a)L_*/(4\pi R_p^2)$ . The planet’s temperature,  $T_p$ , is bounded between the freezing and boiling points of water,  $273 \text{ K} \leq T_p \leq 373 \text{ K}$ . We assume for this calculation that all the starlight is absorbed,  $a = 0$ , to maximize the habitable zone radii. This condition is sufficient to compute the inner and outer habitable zone radii for a star of luminosity,  $L_*$  using general formulae for the orbital radius,  $R_p$ , of a rotating planet at equilibrium temperature,  $T_p$ :

$$R_p = \sqrt{\frac{L_*}{16\pi\sigma T_p^4}}, \quad (11)$$

$$= \frac{1}{2} \left( \frac{T_*}{T_p} \right)^2 r_*. \quad (12)$$

The inner and outer radii of the habitable zone are obtained from (12) with  $T_p = 373$  and  $273 \text{ K}$ , respectively. Effects such as greenhouse warming or low absorption of starlight via high albedo will change these radii by modest factors (Kasting et al. 1993) in opposite directions; for example, the effective temperature of the Earth is  $\sim 255 \text{ K}$  (Orton 2000) and the albedo is  $\sim 0.5$  but the greenhouse effect keeps the surface warm. These corrections are not large enough to change the overall conclusions of this paper, however, and we will subsequently ignore them in the interest of simplicity.

Using (11) to compute the radii bounding the habitable zone,  $\theta_{IWA}$  determines if a telescope of a particular size can resolve the habitable zone for a star at a known distance and luminosity. By examining large samples of stars, it is possible to determine how many have habitable zones that can be observed with a telescope of a given size.

There have been several approaches to deriving samples of stars suitable for direct detection of terrestrial planets. One approach is to take all stars within a complete nearby sample, such as those within 8 pc of the Solar System (Reid et al. 2004) and exclude only the multiple star systems and white dwarfs that would be difficult to observe. Another approach is to apply criteria that maximize the likelihood that some evolved life forms might exist by excluding in addition the very young stars, the evolved giant stars, and stars with a lot of activity. Turnbull (2004) culled 131 such stars from a sample of 2300 within 30 pc concentrating on “Sun-like” F, G, and K stars. A more extensive sample of stars suitable for the SETI program is given by (Turnbull & Tarter 2003) including approximately 18,000 candidates within 2 kpc. This “SETI sample” is important for its inclusion of stars at large distances that could be searched by very large space telescopes, although it excludes stars with spectral types later than K, a potentially strong limit as shown below.

We examined each sample to find stars whose habitable zones can be resolved within the maximum distance for telescopes of different diameters. The observational parameters for these calculations are:  $SN = 10$ , wavelength of  $1 \mu\text{m}$ , spectral resolution  $\Delta\nu/\nu = 0.01$ , detection efficiency  $\eta = 1$ , observing time  $t = 24 \text{ hr}$ .

Table 1 lists the maximum distances and inner working angles derived under these assumptions along with the numbers of stars available for study from the SETI and 8 pc samples. Table 2 shows how the numbers change if the inner working angle is assumed to be  $3\lambda/d_{\text{tel}}$ , typical of the best extant coronagraph designs, and allowing for an overall detection efficiency of 0.25.

Figures 4 and 5 show the cumulative number of stars whose habitable zones could be studied by telescopes of different sizes. The bands of growth delineate the cumulative numbers using either the inner (smaller number) or outer habitable zone radius. The numbers of candidates out to the maximum assumed distances for the different telescope sizes are given in the figure as the average of these two criteria.

The main result is that *the total sample size increases by an order of magnitude when the telescope diameter doubles*. This rapid increase combines both the growth of sample volume with dis-

tance ( $\propto D^3 \propto d_{\text{tel}}^3$ ), and the inclusion of lower luminosity stars at each distance owing to the decrease in inner working angle ( $\theta_{IWA} \propto d_{\text{tel}}^{-1}$ ).

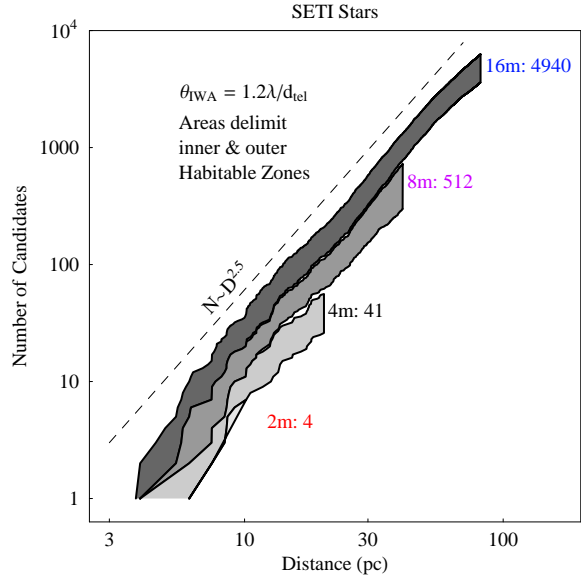


Fig. 4.— Cumulative number of stars from the SETI list vs.  $d_{\text{tel}}$ . Each telescope size shows sample growth in a band between two bounds corresponding to  $\theta_{IWA} \leq R_{\text{in}}$  (lower bound) and  $\theta_{IWA} \leq R_{\text{out}}$  (upper bound). The maximum detection distance forms the right hand boundary of each sample. The numbers next to each diameter are the mean numbers of candidates between the two bands out to the maximum distance. The dashed line shows the power law  $N \sim D^{2.5}$ .

Figure 4 indicates that the number of observable stars increases approximately as  $\sim D^{2.5}$  for any telescope, the requirement that the stars at larger distances are more luminous with larger habitable zones mitigating the otherwise strong  $D^3$  increase of the total sample size. Assuming that this power law is representative for larger distances than 8 pc, we can extrapolate the numbers in columns 4 and 5 of Table 2 to the maximum distance for each telescope to estimate the total number of dwarf stars available. This extrapolation appears in the last column of the table.

These figures represent ideal observations, discounting operational inefficiencies, assuming the planet will be at maximum elongation at the time of an observation, ignoring additional background



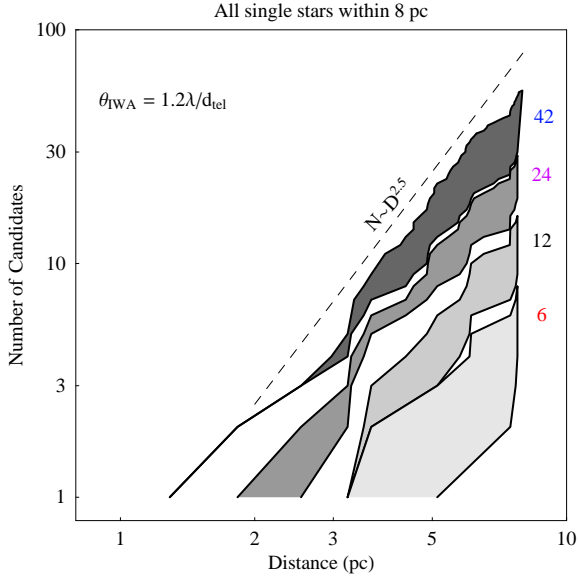


Fig. 5.— Same as Fig. 4 for the complete sample within 8 pc.

from the presence of interplanetary dust in the distant planetary system, and assuming perfect starlight elimination. If the interplanetary dust in distant planetary systems is typically as strong as it is locally, the effect will be to triple the amount of background light per observation on average in (8):  $I(\nu, z) \rightarrow 3I(\nu, z)$ , and the increased background effectively decreases  $D_{max}$  by a factor of  $(1/3)^{1/4} = 0.8$ , decreasing the sample size by about a factor of  $(1/3)^{2.5/4} = 0.5$ . If  $10^{-9}$  of the starlight leaks into the image of the planet the background increases by nearly an order of magnitude, further limiting the observing distance by a factor 0.56 and decreasing the sample size by a factor of more than four.

The inner working angle is a linear function of observing wavelength. We adopted  $\lambda = 1 \mu\text{m}$  as the minimum wavelength of interest to pick up spectral features, but it is obvious from Figure 1 that doubling or tripling this wavelength would be an enormous benefit to search for all the molecular signatures of life. Doubling the wavelength would decrease the sample size by another factor of about two.

Moreover, it is unlikely that a telescope whose inner working angle just resolves the inner habitable zone will be adequate to observe exoplanets

around any one star owing to the relatively small fraction of the projected orbit that will subtend large angular displacements for typical orbital inclinations (Brown 2005; Brown et al. 2007). Realistically,  $\theta_{IWA}$  will have to be much smaller than  $\theta_{IHZ}$  to ensure a good chance of observing the planet in most cases.

Each of these effects will decrease the sample sizes in the tables by factors of a few, and it is clear that the numbers in the tables might be more than an order of magnitude too large for the practical problem of life signatures.

On the other hand, the range for terrestrial-mass planets thought to be suitable for life extends to  $10 M_{\oplus}$ , meaning the observed area of the planet in (4) will be about  $10^{2/3} \approx 5$  times larger than  $\pi R_E^2$ , increasing the sample size by about a factor of 7 ( $N \propto D^{2.5} \propto R^{2.5} \propto M^{2.5/3} = 10^{2.5/3} \approx 7$ ). This factor would boost the numbers in the tables to offset the decreases from other effects above. Furthermore, adopting 24 hr as the limiting integration time could also be too conservative. For an integration time of 100 hr, the distance limit would increase by  $(\frac{100}{24})^{1/4}$ , and the sample size by  $(\frac{100}{24})^{2.5/4} = 2.4$ .

These uncertainties show why refinements to some of these estimates, for example using the greenhouse effect to increase the size of the habitable zone slightly or trying to estimate the exozody background precisely, can complicate the analysis without bringing any greater insight into the likelihood of detecting life-bearing planets. Moreover, the assumptions used here are optimistic about technological advances for observing exoplanets. There are no margins built in to the assumptions that all the starlight is rejected, there is no exo-zodiacal background, the detection efficiency is nearly ideal, and there is sufficient resolution when the inner working angle is equal to the size of the habitable zone. The numbers of candidate stars listed in Table 2 only take into account margins for  $\theta_{IWA}$  and detection efficiency, and we believe they may safely be taken as upper limits to the number of observable stars for a given telescope diameter, allowing for some margin in the uncertainties of the properties of exoplanets.



#### 4. Use of an External Occulter

One way to increase the sample size for small telescopes is to use an external occulter to provide a small inner working angle independent of the telescope aperture. Tables 1 and 2 and Figures 4 and 5 show that the sample size increases approximately linearly with the telescope diameter at a fixed distance (the 8 pc sample) owing to the decrease of  $\theta_{IWA}$ .

Cash (2006) has proposed a novel concept to use a large shaped screen at some distance from a space telescope to block the starlight and allow the telescope to study emission from exoplanets near the star. He provides approximate formulae to estimate the size and distance of an occulter for a given  $\theta_{IWA}$  and telescope size. To double the size of the sample for a 4 m telescope would require an occulter giving the same inner working angle as an 8 m,  $\theta_{IWA} = 30$  mas. Using Cash' formalism, adopting  $\theta_{IWA} = 30$  mas with petal parameter  $n = 3$  and a contrast ratio (planet/starlight) of  $10^{-10}$ , the occulter would have to be 60 m across at a distance of at least 400,000 km from the telescope. Such an occulter would double the sample of a 4 m telescope by increasing the number of stars whose habitable zones could be resolved. This increase would come at the cost of a large occulter placed far from the telescope precisely in line with the star.

This example shows that the gain from using a larger telescope comes about mainly from the rapid increase in sensitivity with aperture size,  $d_{tel}^{-4}$ , and the rapid increase in sample size owing to the larger volume probed:  $N \sim D^{2.5} \sim d_{tel}^{2.5}$ . The use of an external occulter helps mitigate the technical demands of creating a nearly perfect coronagraph, although it will drive some very strong technical demands of its own—alignment of a  $\sim 60$  m structure at 400,000 km from a space telescope and moving it around to sample different stars will be no mean feat. Large telescopes will still have an enormous advantage for searching for signs of life on exoplanets.

#### 5. Spectra of Transiting Exoplanets

It is possible to distinguish very slight differences in the light curve at different wavelengths as an exoplanet transits the face of its central star. These differences result from transmission

spectrum of the star through the planet's atmosphere making the apparent size of the planet larger at wavelengths where the atmosphere is opaque. Charbonneau et al. (2002) and Vidal-Madjur et al. (2003, 2004) demonstrated the utility of this method by detecting sodium, hydrogen, oxygen, and carbon in the extended atmosphere of the transiting exoplanet, HD 209458b, using the STIS spectrograph on 2.4 m Hubble Space Telescope. Tinetti et al. (2007) also used the Spitzer Space Telescope in a similar way to detect H<sub>2</sub>O in HD 189733b. Transits provide an alternative way to look for the signatures of life in exoplanets (Seager & Sasselov 2000).

As a planet passes across the face of a star, the starlight dims by approximately the ratio of the area of the planet to that of the star,  $\Delta_p \approx \pi r_p^2 / \pi r_*^2$ , where we ignore the modest effect of limb darkening. If the scale height of the atmosphere is  $h_{atm}$  and an atmospheric absorption feature has the effect of blocking all light to  $x$  scale heights above the surface, there will be a small difference in the depth of the light curve viewed at the wavelength of the feature:

$$\Delta_{atm} - \Delta_p = \frac{(r_p + x h_{atm})^2 - r_p^2}{r_*^2}, \quad (13)$$

$$\approx \frac{2x h_{atm} r_p}{r_*^2}, \quad (14)$$

where the approximation assumes  $x h_{atm} \ll r_p$ . For the Earth crossing the face of the Sun seen from afar, this an excellent approximation:  $h_{atm} \approx 9$  km,  $r_p \approx 6400$  km, and  $\Delta_{atm} - \Delta_p = 2 \times 10^{-7}$  for  $x = 1$ . The scale height of the atmosphere depends on the density and temperature of the planet through the usual thermodynamic relation:

$$h_{atm} = \frac{k T_p}{\bar{\mu} g}, \quad (15)$$

$$= \frac{3 k T_p}{4 \pi G \bar{\mu} \rho r_p}, \quad (16)$$

where  $g$  is the gravitational acceleration at the planet's surface,  $\bar{\mu}$  is the mean molecular mass, and  $\rho$  is the mean density of the planet<sup>2</sup>. Recast-

<sup>2</sup>The density of a planet increases slightly with mass as the interior equation of state changes (Seager et al. 2007), but the effect is small enough to be ignored at this level of approximation.

ing (14) in terms of the density:

$$\Delta_{atm} - \Delta_p \approx x \frac{3kT_p}{2\pi G \bar{\mu} \rho r_*^2}. \quad (17)$$

This result shows somewhat non-intuitively that the atmospheric signature for a planet in the habitable zone is independent of the planet's size; to first order, it depends only on the density and temperature, the latter of which lies between the freezing and boiling points of water, thus bounding the range of possibilities. The stronger gravitational field of larger planets decreases the scale height to compensate for the increase in the planet's radius.

The number of scale heights for the effective cross section,  $x$ , depends on the strength of the absorption lines. In the Earth's atmosphere, the strength of the absorption lines is normally expressed in terms of the vertical optical depth from the ground to space. For a molecule whose number density,  $n_i$ , as a function of height,  $y$ , is exponential with scale height,  $h_{atm}$ , and absorption cross section per molecule,  $\sigma_i$ , the vertical optical depth is  $\tau_0 = \int_0^\infty n_i \sigma_i \exp(-y/h_{atm}) dy = n_i \sigma_i h_{atm}$ . Then the optical depth through the atmosphere along a line with an impact parameter  $x$  scale heights above the surface is given by:

$$\tau(x) = \tau_0 \int_{-\infty}^{\infty} e^{-\left(\sqrt{(x+r'_p)^2 + y^2} - r'_p\right)} dy \quad (18)$$

$$= 2\tau_0 e^{r'_p} (r'_p + x) K_1(r'_p + x), \quad (19)$$

$$\approx \tau_0 \sqrt{2\pi} (r'_p + x)^{\frac{1}{2}} e^{-x} \quad (20)$$

where  $r'_p = r_p/h_{atm}$ ,  $K_1$  is a modified Bessel function, and the approximation assumes  $r'_p + x \gg 1$ . The value of  $x$  that gives the effective atmospheric cross section for any absorption line seen in transit is the solution to (20) that gives  $\tau(x) = 1$ . For  $r'_p \gg x$ , the solution is:

$$x \approx 0.92 + \frac{1}{2} \ln \left( \frac{r_p}{h_{atm}} \right) + \ln(\tau_0) \quad (21)$$

$$\approx 4.20 + \ln(\tau_0) \text{ for } r'_p = \frac{6400}{9}. \quad (22)$$

The lines shortward of  $1 \mu\text{m}$  in Fig. 1 have vertical optical depths,  $\tau_0$ , between 0.1 and 1 (Crisp 2000), meaning  $x$  is between 2 and 4. There are very strong  $\text{H}_2\text{O}$  lines at wavelengths of a few microns, in principle giving  $x \sim 10$ , although for

the Earth itself, water vapor is confined to the tropopause within a single scale height, so the lack of vertical mixing means that  $x(\text{H}_2\text{O}) \sim 1$  despite the large  $\tau_0$ . The important result of (21) is that the effective cross section within an absorption line depends on the logarithm of the line optical depth; even order of magnitude uncertainties in the total atmospheric density affect the transit depths mildly.

Detecting the absorption lines in a transit observation means achieving very high photometric accuracy in the difference spectrum in and out of the line. The best photometric accuracy that can be achieved during a transit is if all the starlight is detected with perfect efficiency and the only noise source is the statistical fluctuation of the photon rate as assumed in (7). Using the formalism above for measurement time,  $t_{obs}$ , and assuming the difference of two measurements:

$$\frac{\sigma_{N_\gamma}}{N_\gamma} = \left( \frac{2}{\dot{N}_\gamma t_{obs}} \right)^{1/2}, \quad (23)$$

$$= \left( \frac{\pi}{8h} \frac{\Delta\nu}{\nu} F_*(\nu) d_{tel}^2 t_{obs} \right)^{-1/2}. \quad (24)$$

The total observation time will be the time of a single transit times the number of transits. Viewed from a great distance, the maximum transit time is just  $t_{trans} = 2r_*/v_p = 2r_* \sqrt{R_p/GM_*}$ , and the time for an average transit (i.e. not across the equator) is just one half this value. The number of transits observed during the lifetime of a space mission,  $t_m$ , is just  $n_P = t_m/P$ , with  $n_P$  truncated to an integer. The total observation time is:

$$t_{obs} = n_P t_{trans} \quad (25)$$

$$= t_m \frac{1}{2\pi} \sqrt{\frac{GM_*}{R_p^3}} 2r_* \sqrt{\frac{R_p}{GM_*}} \quad (26)$$

$$= t_m \frac{1}{\pi} \frac{r_*}{R_p} \quad (27)$$

$$= t_m \frac{2}{\pi} \left( \frac{T_p}{T_*} \right)^2 \quad (28)$$

We used (12) to express  $R_p$  in terms of the temperatures to yield another non-intuitive result: the total observation time *decreases* as the stellar effective temperature *increases*. This effect is more than enough to offset the advantage of having a

brighter star with a higher photon rate:

$$SN_{tr} = \frac{\Delta_{atm} - \Delta_p}{\sigma_{N_\gamma}/N_\gamma} \quad (29)$$

$$= x \frac{3kT_p^2 d_{tel}}{4\pi G \bar{\mu} \rho r_*^2 T_*} \left( \frac{1}{h} \frac{\Delta\nu}{\nu} F_*(\nu) t_m \right)^{1/2} \quad (30)$$

$$\propto \frac{T_p^2}{r_*^2 T_*^{1/2}} \frac{d_{tel}}{D} \quad (31)$$

To derive (31), we note that for stars hotter than the Sun, an observing wavelength of  $\sim 1 \mu\text{m}$  is nearly on the Rayleigh-Jeans part of the stellar spectrum, meaning the flux density is linearly proportional to the temperature:  $F_*(\nu) \propto \frac{2kT_*}{\lambda^2}$ . Because the stellar radius,  $r_*$ , increases with stellar temperature, this result shows that the signal-to-noise ratio for transit observations of terrestrial planets in the habitable zones around stars increases rapidly with decreasing stellar temperature: small, light stars are strongly favored over massive stars at all distances, both because the transit depths are larger and the observation times are longer, more than offsetting the increased photon rate with increasing stellar temperature. This is a general result that also applies to the case of detecting planetary transits in general, not just the highly challenging observation of atmospheric lines.

Notice that the assumptions used to arrive at (30) are for the best case of maximum transit time and perfect detection efficiency, and there is even a slight increase in the observing time if the number of transits is not truncated to an integer; this result is the best we can do.

We can apply (30) to the samples described in §3 above to find the number of stars where the atmospheric signatures can be detected through transit experiments. Table 3 gives the results. The I magnitudes were used to calculate the photon rates. The 8 pc sample clearly limits the number of potential low luminosity stars for telescopes larger than a few meters. If the growth in sample size vs. telescope diameter is the same for the 8 pc sample as for the SETI sample, we can extrapolate the 8 pc sample numbers to give the results in the sixth column.

The difficulty of using transits to detect atmospheric features is illustrated by evaluating (30) for the Earth/Sun system at a distance of 10 pc.

A single transit of the Earth across the diameter of the Sun takes 16 hours during which an 8 m telescope would capture  $3 \times 10^{14}$  photons at a spectral resolution of  $\Delta\nu/\nu = 0.1$  at  $1 \mu\text{m}$ . The fractional uncertainty in the difference in light curves at two frequencies would be  $\sigma_{N_\gamma}/N_\gamma = 8 \times 10^{-8}$ , yielding a signal-to-noise ratio of 10 on for a feature with  $\tau(h_{atm}) = 1$  and  $x = 4$ , such as the oxygen lines. Since this spectral resolution is too coarse for most features of interest and the telescope is large, it will be probably be impossible to detect signatures of more distant Earths using transits at these wavelengths. However, large telescopes should be able to detect deep water features with  $\tau(h_{atm}) \sim 10^4$  at wavelengths of a few microns with sufficient collecting area, if the water vapor extends throughout the atmosphere, unlike the situation on Earth.

The greater complication with this technique, however, is that the orbital plane of the planet must be aligned with the line of sight for a transit to be observed. The a priori probability of alignment, assuming orientations uniformly distributed within the celestial sphere and requiring only that the planet graze some part of the stellar surface, is:

$$f = \frac{r_*}{R_p}, \quad (32)$$

$$= 2 \left( \frac{T_p}{T_*} \right)^2, \quad (33)$$

where we have used (12) to derive (33). The fraction,  $f$ , is much less than unity even for cool stars, meaning we would need many candidate stars to ensure that even a few transiting planets would be observed. The final column in Table 3 is expected number of transiting planets that would be discovered in the hot sample ( $T_p = 373 \text{ K}$ ):  $\langle n_p \rangle = \sum_i f_i$  based on extrapolating the total number to match the trend in the SETI sample. It shows that for a large telescope, there is a good chance of seeing a few transiting planets around low-mass stars in the Solar neighborhood.

Table 3 again points to the great advantage that large telescopes have for studying transiting exoplanets. An 8 m telescope could yield of order 20 transiting planets of terrestrial mass around low-mass stars in the Solar neighborhood, and a 16 m would yield more than 700. The actual number of candidates needed to ensure the detection of a

life-bearing planet is treated in the final section.

## 6. Likelihood of Life Bearing Planets

The number of life-bearing planets that can be detected in a survey will depend on the fraction of accessible candidate stars with an Earth-like planet in the habitable zones around the star as well as likelihood that the planets develop life quickly enough so that it starts to dominate the planet's atmospheric chemistry. This fraction is conventionally called  $\eta_{\text{Earth}}$ .<sup>3</sup>

One estimate of the likelihood that a planet will be found in the habitable zone around a star can be derived from the fraction of stars with known exoplanets and the distribution of their orbital semi-major axes. There are presently 244 known exoplanets<sup>4</sup>, all much more massive than Earth, whose orbital parameters have been estimated. Figure 6 shows the distribution of semi-major axes of this sample. The range spans approximately 2.5 orders of magnitude. In these logarithmic units, the habitable zone as defined by (11) is 0.27, about 10% of the range. Because these exoplanets have been found in only 15% of the stars surveyed, the empirical chance of finding a massive exoplanet in the habitable zone around a star is 1.5%. If this analysis also applies to terrestrial-mass planets, a sample of order 100 stars would be required to guarantee ( $1\sigma$ ) at least one terrestrial planet in the habitable zone around a star.

This estimate could easily be too low for the problem at hand, however. There are at least eight planets in the Solar System, of which three, Venus, Earth, and Mars, might be capable of supporting life if they are within the habitable zone. The empirical chance of detecting massive exoplanets may be lower than the chance of finding a terrestrial planet, if the Solar System is typical. If planetary systems normally contain several planets of terrestrial mass,  $0.5 - 10 M_{\oplus}$ , the chance that one will be in the habitable zone rises considerably. The microlensing detection of a  $5.5 M_{\oplus}$  planet around an M dwarf (Beaulieu et al. 2006) suggests that terrestrial planets may be more common around low

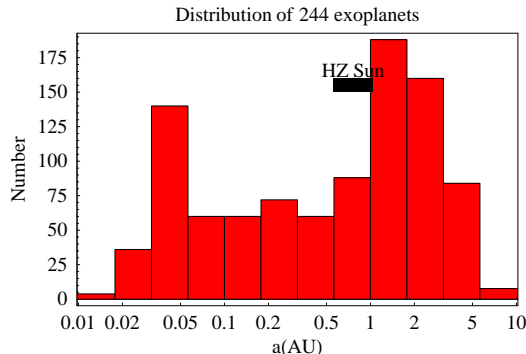


Fig. 6.— The distribution of the semi-major axes of 244 known exoplanets is shown along with the size of the habitable zone around the Sun. Although the location of the habitable zone for each candidate will differ from that of the Sun, the size will be the same in logarithmic units.

mass stars than the empirical frequency of more massive planets. An optimist might say that every planetary system will have a planet within the habitable zone, although whether it can support life would depend on its mass; in the solar system, only about 1/3 of the known planets are in the right range.

How likely is it that life has arisen and evolved to the stage where the atmospheric chemistry reflects its presence? On Earth, life arose quickly then took more than 3.5 billion years to produce enough oxygen via photosynthetic organisms to change the atmosphere in a way we would recognize today (Kasting & Catling 2003, and references therein). The oxygen would disappear from the atmosphere in few million years if life were to cease, and  $\text{CO}_2$  would dissolve in the oceans within a few thousand years, eliminating the most prominent atmospheric signature of organisms on Earth. It required a series of unlikely accidents for Earth to alter its atmosphere, suggesting that it may not occur easily on other planets (Ward & Brownlee 2000).

Thus, an apriori estimate of the fraction of stars with life-bearing planets depends entirely on how much faith we have that all the circumstances are favorable, that is the number of apparent miracles we are willing to believe. If all stars have planetary systems (but only 15% have massive planets), and all planetary systems have at least one

<sup>3</sup>There are various definitions of  $\eta_{\text{Earth}}$  in the literature that may not require that the planet is in the habitable zone nor that it has developed life; the definition here is more demanding.

<sup>4</sup><http://exoplanet.eu/catalog-all.php>

Earth-like planet within the habitable zone, and this planet always evolves life to dominate its atmospheric chemistry, then nearly 100% of the suitable stars (i.e. older than 3 billion years, etc.) will have planets for us to study, i.e.  $\eta_{\text{Earth}} \sim 1$ .

On the other hand, if only 15% of stars typically have planetary systems of which the likelihood of an Earth-like planet in the terrestrial zone is only 30% and the chance of evolving life is less than 1, then  $\eta_{\text{Earth}} < 0.05$ , and it may be much less than this value if the sequence of events leading to life-signatures in the atmospheric spectra are more rare than common; many of the low mass stars making up the majority of the complete 8 pc sample are likely to be too young to have evolved life as on Earth (Reid et al. 2007). A pessimist might conclude that  $\eta_{\text{Earth}} \ll 0.01$ .

We believe that a pragmatic approach to the study of life-bearing exoplanets will require more than 100 candidate stars to yield at least one with the characteristics we seek, requiring a large ( $> 8$  m) space telescope. A very large space telescope of order 16 m diameter would have thousands of candidate stars to study and, while technically challenging to build, would also be an excellent tool for examining exoplanets found by other means, such as spectra-photometry of the transits discussed in §5.

The range of uncertainty will narrow considerably when the results of the Kepler mission to find Earth-like planets around distant stars are known in a few years. However, Kepler is observing more than  $10^5$  distant ( $> 1$  kpc) stars, very few of which will be close enough to look for atmospheric signatures. In the absence of very large space telescopes to find and study nearby stars, it will still leave open the question about the likelihood of life outside of the Solar system.

I am grateful to Robert Brown, Peter McCullough, Marc Postman, Kailash Sahu, David Soderblom, and Jeff Valenti for their advice and to Mike Hauser and Matt Mountain for encouragement to pursue this work. This research was supported by NASA through its contract to AURA and the Space Telescope Science Institute.

## REFERENCES

- Agol, E. 2007, MNRAS, 374, 1271.
- Beaulieu, J.-P. et al. 2006, astro-ph/0601563.
- Beichman, C. A. et al. 2006, ApJ, 639, 1166.
- Born M. and Wolf E. (1999). *Principles of optics*. Seventh edition, Cambridge University Press, Cambridge, UK.
- Brown, R. A. 2005, ApJ, 624, 1010.
- Brown, R. A., Shaklan, S. B., and Hunyadi, S. L. 2007, *Coronagraph Workshop 2006*, JPL Publication 02-02 7/07, W. A. Traub ed. Pasadena:JPL, p. 53.
- Cash, W. 2006, Nature, 442, 51.
- Charbonneau, D., Brown, t. M., Noyes, R. W., and Gilliland, R. L. 2002, ApJ, 568, 377.
- Crisp, D. 2000, in *Allen's Astrophysical Quantities*, Fourth edition, (AIP Press, Springer-Verlag, New York), p. 268.
- Ehrenreich, D., Tinetti, G., Lecavelier des Etangs, A., Vidal-Madjar, A., and Selsis, F. 2006, A&A, 448, 379.
- Guyon, O., Pluzhnik, E. A., Kuchner, M. J., Collins, B., and Ridgway, S. T. 2006, ApJS, 167, 81.
- Kaltenegger, L., Traub, W.A., Jucks, K.W. 2007, ApJ, 658, 598.
- Kasting, J. F. and Catling, D. 2003, ARA&A, 41, 429.
- Kasting, J., Whitmire, D., and Reynolds, R. 1993, Icarus, 101, 108.
- McCullough, P. R. 2006, astro-ph/0610518.
- Orton, G. S. 2000, in *Allen's Astrophysical Quantities*, Fourth edition, (AIP Press, Springer-Verlag, New York), p. 300.
- Reid, I. N., Turner, E. L., Turnbull, M. C., Mountain, M., and Valenti, J. A. 2007, astro-ph/0702420.
- Reid, I. N., Cruz, K. L, Allen, P., Mungall, F., Kilkenny, D., Liebert, J., Hawley, S. L., Fraser, O. J., Covery, K. R., Lowrance, P., Kirkpatrick, J. D., and Burgasser, A. J. 2004, AJ, 128, 463.
- Russell, H. N. 1916, ApJ, 43, 173.
- Sagan, C., Thompson, W. R., Carlson, R., Gurnett, D. and Hord, C. 1993, Nature, 365, 715.
- Seager, S., Ford, E. B., and Turner, E. L. 2002, SPIE, 4835, 79.
- Seager, S., Kuchner, M., Hier-Majumder, & Militzer, B. 2007, astro-ph/0707.2895v1.
- Seager, S. and Sasselov, D. D. 2000, ApJ, 537, 916.
- Seager, S., Whitney, B. A., and Sasselov, D. D. 2000, ApJ, 540, 504.
- Tinetti, G., Vidal-Madjar, A., Liang, M.-C., Beaulieu, J.-P., Yung, Y., Carey, S. Barber, R. J., Tennyson, J., Ribas, I., Allard, N. et al. 2007, Nature, 448, 169.
- Turnbull, M. C. 2004, *The Search for Habitable worlds: From the terrestrial Planet Finder to SETI*, PhD Thesis, U. Arizona.
- Turnbull, M. C. and Tarter, J. C. 2003, ApJS, 145, 181.
- Turnbull, M. C., Traub, W. A., Jucks, K. W., Woolf, N. J., Meyer, M. R., Gorlova, N., Skrutskie, M. F., and Wilson, J. C. 2006, ApJ, 644, 551.
- Traub, W. A. and Jucks, K. W. 2002, GMS, 130, 369.
- Vidal-Madjar, A. et al. 2003, Nature, 422, 143.
- Vidal-Madjar, A., Désert, J.-M., Lecavelier des Etangs, A., Hébrard, G., Ballester, G. E., Ehrenreich, D., Ferlet, R., McCormell, J. C., Mayor, M., and Parkinson, C. D. 2004, ApJ, 604, 69.
- Ward, P. D. and Brownlee, D. 2000, *Rare Earth*, Copernicus Springer-Verlag:New York.

TABLE 1  
SAMPLE SIZES WITH IDEAL TELESCOPES<sup>a</sup>

$d_{\text{tel}}$ m	$\theta_{IWA}$ mas	$D_{\text{max}}$ pc	n(SETI)		n(8pc)	
			IHZ <sup>b</sup>	OHZ <sup>b</sup>	IHZ <sup>b</sup>	OHZ <sup>b</sup>
2	123	10	2	7	4	8
4	62	20	26	56	9	16
8	31	41	300	725	19	29
16	15	81	3607	6272	30	55

$$^a\theta_{IWA} = 1.2 \frac{\lambda}{d_{\text{tel}}} @ 1 \mu\text{m}, \eta = 1, t = 24 \text{ hr}, \frac{\Delta\nu}{\nu} = 0.01$$

$$^b\theta_{IWA} \leq R_p(\text{IHZ}) \text{ or } R_p(\text{OHZ})$$

TABLE 2  
SAMPLE SIZES WITH PRACTICAL TELESCOPES<sup>a</sup>

$d_{\text{tel}}$ m	$\theta_{IWA}$ mas	$D_{\text{max}}$ pc	n(SETI)		n(8pc)		$\langle n(\text{all}) \rangle^b$
			IHZ	OHZ	IHZ	OHZ	
2	309	6.8	0	0	1	1	1
4	155	13.5	3	10	3	7	18
8	77	27	18	78	7	14	222
16	39	54	241	1092	14	22	2155

$$^a\theta_{IWA} = 3 \frac{\lambda}{d_{\text{tel}}} @ 1 \mu\text{m}, \eta = 0.25, t = 24 \text{ hr}, \frac{\Delta\nu}{\nu} = 0.01$$

$$^b\text{Extrapolate 8pc: } n(\text{all}) = 0.5(n_{\text{IHZ}} + n_{\text{OHZ}})(D_{\text{max}}/8 \text{ pc})^{2.5}$$

TABLE 3  
SAMPLE SIZES FOR TRANSIT DETECTIONS<sup>a</sup>

$d_{\text{tel}}(\text{m})$	n(SETI)		n(8pc) <sup>b</sup>		$n_{\text{extra}}(8\text{pc})^d$	$\langle n_p \rangle(8\text{pc})^d$
	$R_{\text{IHZ}}^b$	$R_{\text{OHZ}}^c$	$R_{\text{IHZ}}$	$R_{\text{OHZ}}$	$R_{\text{IHZ}}$	
2	0	1	3	19	19	0.46
4	3	33	22	71	71	1.7
8	40	256	75	87	550	21
16	284	942	87	90	2026	744

$$^a\Delta\nu/\nu = 0.01, 10\sigma, 5 \text{ yr}, \rho = 5.5 \text{ g cm}^{-3}, \bar{\mu} = 30 \text{ amu}, x = 4.2$$

$$^b\text{Numbers restricted by 8 pc sample limit}$$

$$^c\text{Planet orbit at inner or outer HZ: } T_p = 373 \text{ or } 273 \text{ K}$$

$$^d\text{Extrapolated using the trend of the SETI sample}$$